Diffusion of particles interacting via long-range and oscillating forces in one dimension

Filip Krzyżewski and Magdalena A. Załuska-Kotur*
Institute of Physics, Polish Academy of Sciences, Al. Lotników 32/46, 02-668 Warsaw, Poland
(Received 25 May 2009; revised manuscript received 3 August 2009; published 2 October 2009)

Collective diffusion coefficient in a one-dimensional lattice gas adsorbate is calculated using variational approach. Particles interact via either a long-range, or a long-range electron-gas-mediated (for a metallic substrate), or a 12-6 Lennard-Jones interaction. Diffusion coefficient as a function of the adsorbate density strongly depends on the relationship between the substrate lattice constant and the characteristic length of the interparticle interaction potential (which determines positions of the potential energy minima). The diffusion coefficient at fixed density as a function of the interaction characteristic length has an oscillating character due to the interplay between the interparticle distances allowed by the substrate lattice structure and the average interparticle distances which minimize the total interaction energy.

DOI: 10.1103/PhysRevB.80.155410 PACS number(s): 68.43.Jk, 02.50.Ga, 66.30.Pa

I. INTRODUCTION

Manipulation of single atoms and self-assembly techniques are very useful methods in nanotechnology. Self-assembly is determined by interatomic interactions, which at the crystal surfaces can be direct or indirect (i.e., induced by the substrate). Recent studies on adatom arrangement and their dynamics on metallic surfaces show that they experience an indirect electron-gas-mediated interactions. Electronic surface states are a source of a long-range interactions, which decay with the interparticle distance r as $1/r^2$ and often have an oscillatory character.[1–15] Such interactions between adatoms lead to their self-alignment in rows[14–20] or in hexagonal structures.[6,12,21–25] This ordering mechanism is a good candidate to be used for constructing and manipulating nanostructure systems. Linear arrangements have unique magnetic and/or electronic properties. The ordering dynamics and a stability of an ordered structure depend on diffusion of adatoms on the surface, while diffusion in a system of adatoms is controlled by interactions between them.

The collective or chemical diffusion coefficient of adsorbed species characterizes a relaxation of the local density fluctuations in a many-particle system. It involves jumps of individual atoms from one binding site to another and describes their collective movement. Theoretical description of the collective diffusion process is a complicated many-body problem and various approaches have been applied to it, ranging from analytic ones based on master, Fokker-Planck, or Kramers equations to numerical Monte Carlo or molecular dynamics simulations. An important background is provided in the works of Reed and Ehrlich,[26] an early summary by Gomer,[27] and in reviews by Danani *et al.*[28] and Ala-Nissila *et al.*[29] The variational approach to the collective diffusion problem, used here, was developed in a series of works[30–37] and was shown to be a very efficient tool to analyze collective diffusion problems for various types of interparticle interactions for homogeneous or inhomogeneous substrates either in one or two dimensions.

We have shown in Ref. 37 that the long-range repulsive interactions can be responsible for rapid macroscopic rearrangements of adatoms upon minuscule adsorbate density changes. We have shown that the adsorbate density dependent diffusion coefficient has peaks at densities corresponding to any ordered phase in a devil staircase phase diagram. It is well known[38,39] that the devil staircase structure emerges when the interparticle interaction potential is repulsive and decays faster than $1/r$. It has been shown, one the other hand, that adatoms on metallic surfaces often interact via forces with oscillating in r potential energies.[1–15] They exhibit a $1/r^2$ decay modified by Friedel oscillations of the electron-gas correlation function, meaning that particles attract each other at some distances and repel at others. Such a distance dependence of the interparticle interactions should, in principle, result in a diffusion character similar to that already investigated for pure $1/r^2$ repulsion. On the other hand, the oscillating interaction potential has local minima. Similarly, a minimum is present also for the interaction of the Lennard-Jones type. The question on how the presence of such a minimum (or minima) affects the diffusion kinetics in a many particle system arises. In particular, the question on how the oscillating character of the interactions decaying like $1/r^2$ modifies diffusion in comparison with the interactions decaying like $1/r^2$ monotonically is interesting.

It is well known that the shape of interaction potential, in particular, the existence of its attractive parts, is very important for the static behavior of the system. Systems with attractive interactions form stable clusters of ordered phases, whereas ordering via repulsion is always global—it affects the entire system. Consequently, an ordered phase due to attractive interactions occurs for a wider range of adatom densities so it is easier to observe experimentally.[10,12,21,25] Such difference in static properties has to affect the dynamic behavior too, so it should affect also the diffusion process. For example, a fast collective diffusion in ordered structures[36,37] leads to a fast reorganization of the adsorbed layer.

In this work we compare three types of interactions: monotonically decaying like $1/r^2$, the oscillating ones decaying like $1/r^2$ with electron-gas-mediated oscillations, and the 12-6 Lennard-Jones interactions. We analyze the influence of the shape of the interaction potential on the diffusion coefficient at different adsorbate densities. Magnitude of the diffusion coefficient depends on several parameters, most of them related to the character and strength of the interparticle interaction. In what follows we analyze how periodic in r variation in the potential superimposed on the $1/r^2$ decay influences diffusion. We show that for systems of particles interacting via oscillating electron-gas-mediated forces or via

forces corresponding to the 12-6 Lennard-Jones potentials, the diffusion process depends sensitively on the ratio between the distance r at which the potential has a minimum and the substrate lattice constant. This ratio allows distinguishing between the commensurate and incommensurate type of diffusion kinetics. We show that the diffusion coefficient depends periodically on the characteristic length of the potentials under investigation.

The paper is organized as follows. In Sec. II the approach to the diffusion coefficient calculation is shortly described. Section III contains description of results for electron-gas mediated, oscillation potential, and then for 12-6 Lennard-Jones potential. Section IV summarizes main results of the work.

II. MODEL

System of N particles interacting via long-range forces is distributed homogeneously over a one-dimensional substrate of length L with a lattice constant a. The interaction of two particles at the lattice positions l_i and l_j contributes the potential energy $\varepsilon(al_i-al_j)$ to the total energy of the system. Following Refs. 37 and 38 we consider systems with the pair potential energy $\varepsilon(r)$ decreasing rapidly with r. This justifies to neglecting the next-nearest-particle interactions and accounting only for pair interactions between neighbors no matter how large the intrapair separation al is. The total interaction energy of the system is $\Sigma_l n_l \varepsilon(al)$, where n_l is the number of nearest-neighbors pairs of length l (in units of a), and only l's satisfying the condition $\Sigma_l l n_l = L$ are admitted in the sum. In a grand canonical ensemble approach we let ℓ to vary from 0 to ∞ and keep, instead, the system under fixed external pressure P (in one dimension it is just an external force), which is determined by the condition that the mean nearest-neighbor pair length $\langle l \rangle$ is equal to the inverse of the actual coverage θ,

$$\langle l \rangle = \frac{1}{\theta} = \frac{N}{L}. \tag{1}$$

In such case a probability of a pair of a length l is[37,38]

$$p_\ell(P,T) = Z_1^{-1}(P,T) e^{-\beta \tilde{\varepsilon}(l,P)}, \tag{2}$$

where

$$\tilde{\varepsilon}(l,P) = \varepsilon(al) + aP\ell \tag{3}$$

and

$$Z_1(P,T) = \sum_{l=1}^{\infty} e^{-\beta \tilde{\varepsilon}(l,P)} \tag{4}$$

is a single nearest-neighbor-pair isothermal–isobaric partition function.

Equations (2)–(4) allow determining the thermodynamic properties of the system. In particular, the equation of state, relation between the coverage, pressure, and temperature, is obtained by evaluating the mean nearest-neighbor pair length

$$\langle l \rangle = Z_1^{-1}(P,T) \sum_{l=1}^{\infty} l e^{-\beta \tilde{\varepsilon}(l,P)} = -\frac{1}{\beta a} \left(\frac{\partial \ln Z_1}{\partial P} \right)_T, \tag{5}$$

and identifying it with $1/\theta$. In the low temperature limit the main contributions to this sum come from one or at most two terms only.[37]

Collective diffusion of the system is modeled by a kinetic lattice gas with the particle hopping rates depending on the actual potential energy of the particle. The potential energy landscape is built by the static potential due to the substrate, as experienced by a single particle, and by interactions of the particle with its neighbors. Time evolution of the system is controlled by a set of master rate equations for the probabilities $\mathcal{P}(\{c\},t)$ that a *microstate* $\{c\}$ of a lattice gas occurs at time t,

$$\frac{d}{dt}\mathcal{P}(\{c\},t) = \sum_{\{c'\}} [W(\{c\},\{c'\})\mathcal{P}(\{c'\},t) - W(\{c'\},\{c\})\mathcal{P}(\{c\},t)]. \tag{6}$$

The microstate $\{c\}$ is understood as a set of variables specifying which particular sites in the lattice are occupied and which are not. $W(\{c'\},\{c\})$ is a transition probability per unit time (transition rate) that the microstate $\{c\}$ changes into $\{c'\}$ due to a jump of a particle from an occupied site to an unoccupied neighboring site. Microstates $\{c\}$ and $\{c'\}$ differ here only by the position of a single particle, the one which jumped. For thermally activated jumps the hopping rate depends on the difference between the energy of the system when the hopping particle is at an intermediate position between the sites engaged in the jump and the energy of the system when the particle is in its initial position. The only contributions that do not cancel out in the difference is the energy of the hopping particle in its initial position and its energy in the activated state at the top of the potential barrier which it jumps over. For the particle hopping from the adsorption site specified by a pair of integers (l,s) (i.e., with the nearest neighbors of adsorbed particles being at a distance al and as, respectively, to its left and right) to a neighboring site $(l',s')=(l\pm 1, s\mp 1)$, the potential energy at the initial adsorption site is

$$E_A = E_A^0 + \varepsilon(al) + \varepsilon(as), \tag{7}$$

where E_A^0 is static potential energy at given site due to the interactions with the substrate. The hopping rate can be written as

$$W(\{c\},\{c'\}) = W_{l',s'}^{l,s} = W^0 e^{-\beta[\Delta_{l',s'}^{l,s} - \varepsilon(al) - \varepsilon(as)]}, \tag{8}$$

where

$$W^0 = \nu \exp[-\beta(E_B^0 - E_A^0)] \tag{9}$$

is a hopping rate for an isolated (i.e., noninteracting) particle and ν is an intrinsic attempt frequency. $\Delta_{l',s'}^{l,s}$ is the amount by which the potential energy E_B^0 of the hopping particle at a bridge site between its initial and the final position is modified by interactions with the neighbors at each its side. We parametrize a microstate $\{c\}$ as $\{c\}=[X,\{m\}]$ by selecting one particle as a *reference particle*, denoting its lattice position as

X and specifying positions $\{m\}=\{m_1,m_2,\ldots,m_{N-1}\}$ of all remaining $N-1$ particles with respect to it.[37] $\{m\}$ is referred to as a *configuration*. Master Eq. (6) are linear in set of probabilities $\mathcal{P}(X,\{m\},t)$ and so their lattice Fourier transform with respect to X can be easily done. The result is that k components of the probabilities, $\mathcal{P}_{\{m\}}(k,t)$, evolve in time independently of each other. The rate equations for $\mathcal{P}_{\{m\}}(k,t)$ can be expressed in terms of a k-space microscopic rate matrix $\mathbb{M}(k)$ (with rows and columns labeled by $\{m\}$) containing the individual hopping rates and phase factors like $e^{\pm ika}$. Details can be found in Refs. 34 and 37. The collective diffusion coefficient is related to that eigenvalue $-\lambda_D(k)>0$ (termed the diffusive eigenvalue) of $\mathbb{M}(k)$ which vanishes like k^2 in the limit $k\to 0$. This eigenvalue is then estimated from above in a spirit of a variational principle[34] as

$$\lambda_D(k) \equiv \frac{\tilde{\phi}\cdot[-\mathbb{M}(k)]\cdot\phi}{\tilde{\phi}\cdot\phi} \to -Dk^2, \tag{10}$$

where the $\to$ stands for the $k\to 0$ limit and $\tilde{\phi}$ and ϕ are variational trial left and right eigenvectors, respectively, of $\mathbb{M}(k)$ corresponding to the diffusive eigenvalue. It has been shown[34,37] that for a homogeneous substrate the $\{m\}$-th component of the trial left eigenvector has the form

$$\tilde{\phi}_{\{m\}}(k) = 1 + \sum_{j=1}^{N-1} e^{ikam_j}. \tag{11}$$

and that $\phi_{\{m\}}(k)=P^{\mathrm{eq}}_{\{m\}}\tilde{\phi}_{\{m\}}(k)$, where $P^{\mathrm{eq}}_{\{m\}}$ is the probability of the configuration $\{m\}$ in equilibrium.

We calculate the diffusion coefficient D as a ratio (the $k\to 0$ limit is implied)

$$D = -\frac{\lambda_D}{k^2} = \frac{\mathcal{M}(k)}{\mathcal{N}(k)k^2}, \tag{12}$$

of the "expectation value" numerator

$$\mathcal{M}(k) = \sum_{\{m\},\{m'\}}^{\text{no rep}} P^{\mathrm{eq}}_{\{m'\}} W_{\{m\},\{m'\}} \times |\tilde{\phi}^*_{\{m'\}}(k) - \tilde{\phi}^*_{\{m\}}(k)|^2, \tag{13}$$

to the "normalization" denominator

$$\mathcal{N}(k) = \sum_{\{\bar{m}\}} P^{\mathrm{eq}}_{\{\bar{m}\}} |\tilde{\phi}_{\{\bar{m}\}}(k)|^2. \tag{14}$$

Detailed balance condition was used to derive Eq. (13) so each $(\{m\},\{m'\})$ term in it accounts for transitions between $\{m\}$ and $\{m'\}$ in either direction. Therefore, each configuration pair $(\{m\},\{m'\})$ appears in the sum in Eq. (13) only once [as indicated by the comment "no rep" above the sum] in order to avoid double counting. In the grand canonical ensemble approach, mentioned earlier, both $\mathcal{N}$ and $\mathcal{M}$ are functions of P, T, and N. We note in passing that $\mathcal{N}$ and $\mathcal{M}$ are directly related to the diffusion coefficient static (or thermodynamic) and kinetic factor, respectively, which the diffusion coefficient is customarily factorized into.[26,27] The former is controlled only by the static interactions, determining the equilibrium properties of the system, while the latter is also sensitive to the dynamic interactions within the adsorbate and the dynamic interactions with the substrate, both controlling the rate of an approach to the thermodynamic equilibrium. Certain characteristic features of the density dependence of the static factor, often being signatures of an onset of an organization within the system, may or may not be compensated by the features present in the kinetic factor, resulting in the density dependent diffusion coefficient from which such features may be absent. This issue for long-range repulsive interparticle interaction was examined in detail in Ref. 37.

It was shown[37] that, for the one-dimensional system with long-range interactions, the denominator (14) can be expressed as[37]

$$\mathcal{N}(k=0;P,T,N) = N\frac{\langle l^2\rangle - \langle l\rangle^2}{\langle l\rangle^2}, \tag{15}$$

while the numerator can be written as

$$\mathcal{M}(k;P,T,N) = (ka)^2 N \sum_{\substack{l=1\\ s=2}}^{\infty} W^{l,s}_{l+1,s-1} p_l(P,T) p_s(P,T). \tag{16}$$

The no rep restriction in Eq. (13) results in only the rates of jumps from the left to right to be explicitly present in Eq. (16) [alternatively, expression mathematically equivalent to Eq. (16) with only the right-to-left jump rates explicitly appearing in it can be used].

To evaluate $\mathcal{M}(k)$ using Eq. (16) the potential energy correction due to interactions of the activated particle is needed. One of the simplest models accounting for the activated particle interactions is obtained by realizing that the particle hopping from the adsorption site (l,s) to $(l+1,s-1)$ surmounts a potential energy barrier at a bridge site situated, approximately, at a distance $l+\frac{1}{2}$ and $s-\frac{1}{2}$ from its nearest left and right adsorbed particle neighbor, respectively, and by evaluating the interaction potential energy at the bridge by using $\varepsilon(al)$ generalized to half-integer arguments. Consequently, the potential energy correction due to interactions of a particle at the bridge site between (l,s) and $(l+1,s-1)$ site is

$$\Delta^{l,s}_{l+1,s-1} = \varepsilon\left(al + a\frac{1}{2}\right) + \varepsilon\left(as - a\frac{1}{2}\right), \tag{17}$$

which, used in Eq. (8), leads to the following hopping rate for the left-to-right jumps:

$$W^{l,s}_{l+1,s-1} = W^0 e^{-\beta[\varepsilon(al+a(1/2))+\varepsilon(as-a(1/2))-\varepsilon(al)-\varepsilon(as)]}. \tag{18}$$

Using Eq. (18) in Eq. (16) yields the kinetic factor

$$\mathcal{M}(k;P,T,N) = (ka)^2 \frac{NW^0}{[Z_1(P,T)]^2}\left[\sum_{l=1}^{\infty} e^{-\beta\tilde{\varepsilon}(l+(1/2))}\right]^2, \tag{19}$$

in which the definition of $\tilde{\varepsilon}$ in Eq. (3) is used. Similarly like in $Z_1(P,T)$ in Eq. (4) the main contribution to the sum over l in Eq. (19) comes from one or at most two terms for low enough temperatures but, for a given value of P, these terms

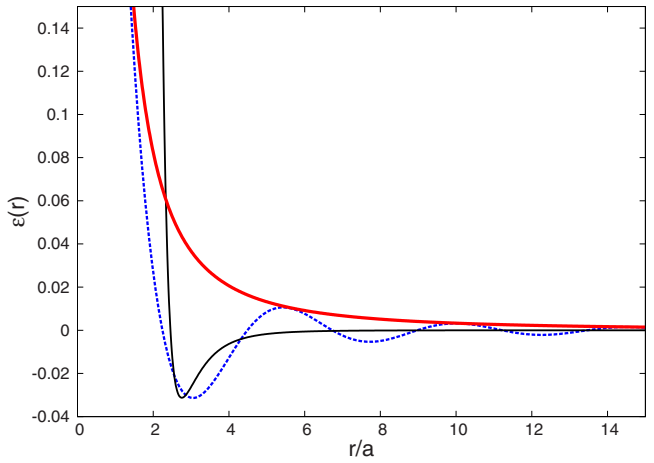

FIG. 1. (Color online) Interparticle interaction potential energies as a function of the interparticle distance r. Thick solid line (red): $\varepsilon_{\text{alpha}}(r)=\alpha/r^2$ with $\alpha/a^2=0.33$ eV; dashed line (blue): the oscillating potential energy in Eq. (20) with $q_F a=0.7$, $\epsilon_F=0.36$, and $\delta_F=-\pi/2$; thin solid line (black): the 12-6 Lennard-Jones potential energy in Eq. (21) with $\sigma/a=2.455$ and $\epsilon_{LJ}=0.031$ eV.

may correspond to different l's than those most significant in Z_1. In general, the sum has to be evaluated numerically.

III. RESULTS

It has been shown that the potential energy of interactions of adatoms adsorbed on metallic surfaces like Cu/Cu(111),[6] Fe/Cu(111),[15] Ce or Co on Cu(111),[9] Fe or Co on Ag(111),[14] and Ce/Ag(111)[21] vary with the interatomic distance r as

$$\varepsilon(r) = -\epsilon_F \left(\frac{2\sin(\delta_F)}{\pi}\right)^2 \frac{\sin(2q_F r + 2\delta_F)}{(q_F r)^2}, \tag{20}$$

where ϵ_F and q_F are, respectively, the Fermi energy and the Fermi wave vector of the surface electrons.[4] Shape of the potential energy depends also on the Fermi-level phase shift δ_F, which for many systems is equal to $-\pi/2$. This value will be used further in our calculations. As it was shown in Ref. 10 formula (20) gives only approximated value of real interparticle potential. In fact its dependence on the distance is more complicated. Moreover metallic substrate mediates also non-negligible three-body interactions between adsorbed adatoms.[5] However in our further calculations we will use two-body interactions in form (20). It will be shown that the diffusion depends only on the main characteristics of the potential shape. Value of the collective diffusion coefficient does not depend so much on the details of the potential shape. In fact there are some similarities in the behavior of the diffusion coefficient even for particles interacting via so different forces as Lennard-Jones and Eq. (20) or $1/r^2$ and Eq. (20).

The interparticle distance dependence of the interaction energy (20) is plotted in Fig. 1 using a dashed line. In this plot parameter $\epsilon_F=0.36$ eV has been chosen, the value of the order of that observed for real substrates. In further calculations of collective diffusion coefficient it is the unitless product $\beta\epsilon_F$ that matters; hence when energy and temperature are rescaled simultaneously we stay with the same diffusion curve. Distance is measured in all calculations in lattice constant a, which at surface, is close to 3 Å, and again it is the unitless product $q_F a$ which decides about the shape of diffusion curves. Potential (20) is compared in Fig. 1 with a long-range purely repulsive potential energy $\varepsilon_{\text{alpha}}(r)=\alpha/r^2$ used in Refs. 37 and 38. The value of the parameter α used in Fig. 1 has been chosen in such a way that the repulsive potential energy curve forms an upper envelope of electron-gas-mediated potential energy (20). Strength of both types of interactions decays with the distance like $1/r^2$, however, whereas the forces corresponding to the α/r^2 potential energy are repulsive at any interatomic separation, the potential energy (20) oscillates, generating attractive forces at some interparticle distances and the repulsive ones at others. Attractive forces in the system lead to the creation of stable structures at the surface and should affect the dynamic properties of the system. We compare here the diffusion kinetics in adsorbates with both types of interparticle interactions and, in addition, in systems in which the interactions correspond to the 12-6 Lennard-Jones potential energy

$$\varepsilon_{LJ}(r) = 4\epsilon_{LJ}\left[\left(\frac{\sigma}{r}\right)^{12} - \left(\frac{\sigma}{r}\right)^{6}\right], \tag{21}$$

typical for interactions between neutral atoms. The parameters ϵ_{LJ} and σ decide about depth and position of the single potential minimum. The Lennard-Jones potential has a repulsive $\propto 1/r^{12}$ wall at short distances, much steeper than $1/r^2$, as it can be seen in the Fig. 1. At larger distances this potential is attractive and, decaying like $1/r^6$, it is weak in comparison with any of the other two. It will be shown, however, that the existence of this attractive part is sufficient for the diffusion kinetics in the system with the Lennard-Jones interactions to be qualitatively similar at some densities to that in systems with oscillating interactions.

A. Diffusion in systems with electron-gas-mediated interactions

It is known[39] that a system of particles with long-range unscreened repulsive interactions orders at $T=0$ at densities (coverages) given by a rational fraction (smaller than 1) when the interaction potential decays faster than $1/r$. The coverage plotted against external potential has a fractal form called a devil staircase.[39] It is also known[38] that systems with interactions decaying faster than $1/r$ but additionally screened to nearest neighbors no matter how far they are (as described in Sec. II) also form ordered $T=0$ phases at coverages equal to $1/n$, where n is any natural number. The "phase diagram" (density vs pressure or the chemical potential) in this case is not as complicated as that for the unscreened interactions—it has no fractal structure. For such a system it is possible to calculate all static properties[38] as well as to investigate fully the collective diffusion kinetics[37] for many models of microscopic kinetics. In general, the collective diffusion coefficient peaks at sufficiently low temperatures at densities at which the system orders (except when sharp drops in compressibility are compensated fully by kinetics for very special models of microscopic kinetics[37]). For

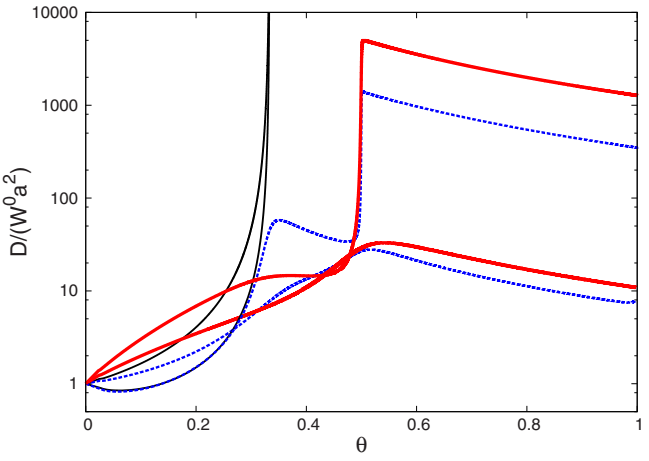

FIG. 2. (Color online) Density dependence of the collective diffusion coefficient divided by the single-particle hopping rate W_0 at temperatures $\beta=1/k_BT=60$ eV^{-1}, $T=193$ K (higher curves) and $\beta=20$ eV^{-1} $T=580$ K (lower curves) for the interaction potential energies plotted in Fig. 1. Thick continuous lines (red): for $\varepsilon_\alpha(r)=\alpha/r^2$; dashed line (blue): for the oscillating potential energy in Eq. (20); thin solid line (black): for the 12-6 Lennard-Jones potential energy in Eq. (21). The interaction potential energy parameters are the same as in Fig. 1.

these densities and for densities around them (at finite temperatures), the diffusion is very fast, meaning that particles have an ability to rearrange quickly when the density changes even by a small amount.

When the interactions are purely repulsive, like for $\varepsilon_{\text{alpha}}(r)=\alpha/r^2$, the rearrangement into an ordered phase occurs for the entire lattice gas at once, the phase transition is of the second order, and formation of ordered domains surrounded by disordered regions with lower or higher densities is not possible. Such possibility opens for systems with interactions like in Eq. (20) which, depending on interparticle distances alternate between repulsion and attraction. When particles attract each other at some distances it is possible to order the system locally even if globally the density is too low for that.[17,21] Note that when particle interact via potential plotted in Fig. 1., $r=3a$ is the preferred interparticle distance (based solely on the total interaction energy considerations), so local ordered domains which are preferentially formed correspond to a local coverage $\theta=1/3$.

In Fig. 2 we compare the coverage dependence of the diffusion coefficient plotted at two different temperatures for the interaction potential energies plotted in Fig. 1. Let us note that the diffusion coefficient plotted in Fig. 2 is divided by hopping rate of the single particle (9), which does not depend on the density and at given temperature is constant. Normalization of all curves by W_0 causes that they all start at $D(0)/W_0=1$ and that curves plotted for lower temperatures lie above curves plotted for higher temperatures. Multiplication by W_0, different for each temperature, should turn over this order. It can be seen in Fig. 2 that the character of the curves corresponding to the interaction potential energies $\varepsilon_\alpha=\alpha/r^2$ and the oscillating one [given in Eq. (20)] is similar at the same temperatures. The only significant qualitative difference between these two cases is seen at and below $\theta=1/3$. The diffusion coefficient for the oscillating interaction exhibits a peak, which is almost invisible for the system with a purely repulsive interaction at the same temperature despite the fact that for purely repulsive interaction the system does order at $\theta=1/3$ at $T=0$. It indicates that the presence of the interparticle attraction for the system with oscillating interaction allows for an ordering corresponding to $\theta=1/3$ already at temperatures much higher than those needed for such ordering with the repulsive long-range interactions only. Attraction, creating the potential energy minimum, is a necessary condition for the formation of the local ordered domains, allowing for their stability. The existence of such domains results in characteristic convex shape of the diffusion curve for densities lower than the ordering density. High diffusion coefficient within such domains aids in their formation because collective diffusion of particles effectively controls the system ability to create ordered phases.[6,9,17,21] With purely repulsive interactions the ordering is possible only globally so the diffusion coefficient peak for $\theta=1/3$, very sharp at $T=0$, is easily smeared out by thermal fluctuations.

We show also in Fig. 2 the diffusion coefficient for the Lennard-Jones interaction. Here, the interactions favor the interparticle distance of about $3a$, almost the same as the oscillating interaction does, so it is not surprising that at low concentrations both interactions result in almost the same value of the diffusion coefficient. At higher concentrations, however, the diffusion kinetics is controlled by a very steep repulsive core at short distances, much steeper for the Lennard-Jones than for any of the remaining two interactions. Consequently, the diffusion coefficient increases to very high values already at $\theta=1/3$. More features unique to the Lennard-Jones interaction will be discussed in Sec. III B.

In general, the character of the density dependence of the collective diffusion coefficient strongly depends on how closely the minima and the maxima of the oscillating interaction potential energy match the distances between particles which occupy the substrate lattice sites. In Fig. 3 the interaction potential energies for several values of q_F are shown. It can be seen that the position of the first minimum moves toward higher interparticle distances with decreasing q_F. Geometrically, the minimum interparticle distance possible is a, the substrate lattice constant, and the overall character of the coverage dependence of the diffusion coefficient is to a major extent determined by the character of the interaction at this particular interparticle distance.

If at the separation a the interparticle interaction is strongly repulsive, as it is for $q_F=0.3/a$, $0.35/a$, $0.7/a$, or $1/a$, then the diffusion coefficient behaves as a function of coverage (for coverages between $\theta\approx 1/2$ and 1), similar to that corresponding to a purely repulsive interaction (as seen already in Fig. 2 for $q_F=0.7/a$): it raises rapidly when the coverage approaches the value $\theta=1/2$ from below, suffers a kink, and then decreases slowly with further increase in θ. This behavior was already analyzed for a purely repulsive long-range interaction in Fig. 9 of Ref. 37. It can be traced back to the behavior of the diffusion coefficient static factor, proportional to $1/\mathcal{N}$ (i.e., proportional to an inverse of an isothermal compressibility), modified by the behavior of the kinetic factor, proportional to $\mathcal{M}$. For these values of q_F the particles avoid occupying the nearest-neighbor sites, so for

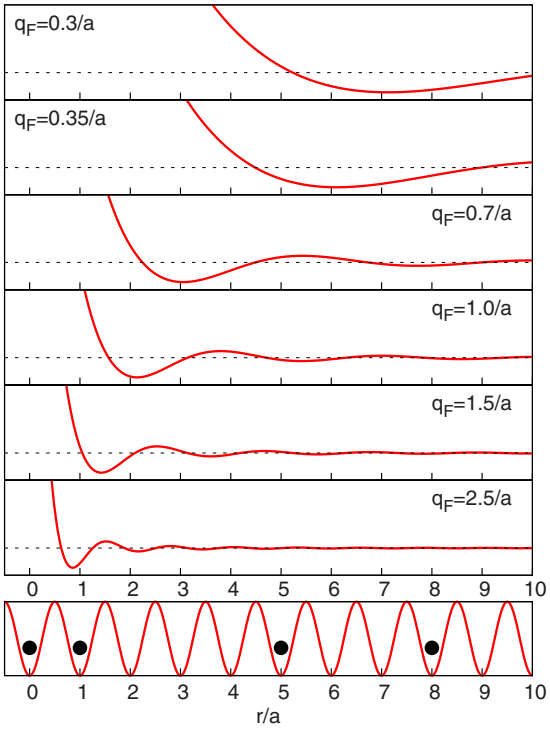

FIG. 3. (Color online) Interparticle potential energies (20) as a function of the interparticle interaction distance r for several values of q_F (from $0.3/a$ up to $2.5/a$) and $\epsilon_F=0.36$ eV

$\theta \approx 1/2$ they preferentially occupy every second lattice site. A substantial additional pressure is needed to compress the system above half occupation of the lattice, the isothermal compressibility is very low, i.e., the static factor goes through a sharp maximum at $\theta=1/2$. The overall shape of the density dependence of the diffusion coefficient is determined, however, by both the static and the kinetic factor. With the hopping rates given in Eq. (18) the high value for interaction potential energy at the interparticle distance a results in a kinetic factor, which also increases sharply at $\theta=1/2$ but does not reach a maximum there. Instead, for $\theta>1/2$ variations in the kinetic factor almost perfectly compensate for the variations in the static factor for these densities. The compensation between both factors for $1/2<\theta \leq 1$ results in the diffusion coefficient, which only slowly decreases as a function of θ over this coverage interval.

The structure observed in Fig. 4 at coverages below $\theta=1/2$ (i.e., at $\theta \approx 1/3$ and smaller) for $q_F a \leq 0.7$ may be understood in a similar way. In these cases the interparticle interaction is strongly repulsive not only at a separation a but also at the next possible one, $2a$, so at coverages close to $\theta \approx 1/3$ the particles preferentially occupy every third site with the resulting compressibility minimum at that coverage. We can see in Fig. 4 that locally, within the coverage interval $0.3<\theta<0.47$, the behavior of the diffusion coefficient for the interactions corresponding to $q_F a \leq 0.7$ is quite reminiscent of that within the interval around $\theta=1/2$ and above it (for the same values of q_F and also $q_F=1/a$): a sharp increase at $\theta=1/3$ is followed by a slow diffusion coefficient decrease with increasing θ (until the singularity at $\theta=1/2$ takes over). For still lower q_F's similar structures are observed in Fig. 4 around $\theta=1/6$ and even 1/7.

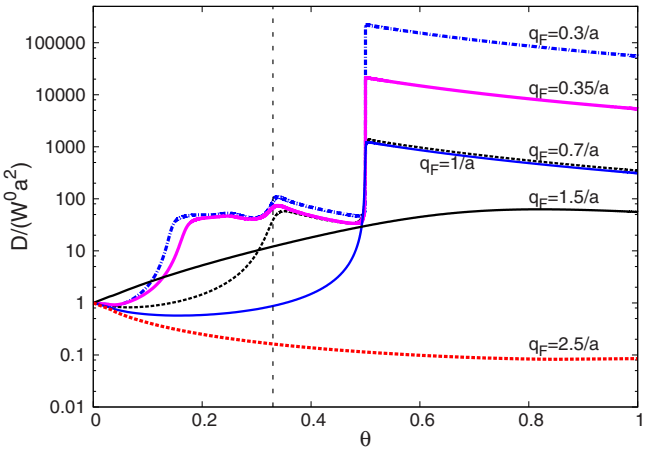

FIG. 4. (Color online) Density dependence of the diffusion coefficient divided by the single particle hopping rate W_0 in the system with oscillating interparticle interaction (20) for several values of q_F (from $0.3/a$ up to $2.5/a$—the same as in Fig. 3), $\epsilon_F=0.36$, and $\beta=60$ eV^{-1}

It was checked that upon increasing q_F gradually up from $0.7/a$ the structure around $\theta=1/3$ in Fig. 4 evolves initially into the locally concave dependence around $\theta=1/3$ and then into the locally convex one, as seen in Fig. 4 for $q_F=1/a$. Further increase in q_F washes out the only remaining structure around $\theta=1/2$; $D(\theta)$ becomes a structureless concave function (as seen for $q_F=1.5/a$) and then it evolves into a convex one (as seen for $q_F=2.5/a$). It is worth noting that the evolution of the $D(\theta)$ from a function with the structure at $\theta=1/2$ for $q_F=1/a$ through the concave structureless function for $q_F=1.5/a$ and then to the convex one for $q_F=2.5/a$ parallels the evolution of $D(\theta)$ observed in Figs. 3 and 4 of Ref. 32 for the short-range interaction changing from the strongly repulsive, through the weakly repulsive, to the attractive one. Indeed, as seen in Fig. 3, the interparticle interaction at a distance a is strongly repulsive for $q_F=1/a$, weakly so for $q_F=1.5/a$ and somewhat attractive for $q_F=2.5/a$.

Convex shape of $D(\theta)$ is characteristic for systems with dominant attractive interparticle interactions, which cause them to bond and to form clusters. When particles stay on average at distances that minimize the total interaction energy, the jump rates are lowered according to Eq. (8), resulting in a decrease in the diffusion coefficient kinetic factor. Diffusion for $q_F=2.5/a$ oscillating interaction decreases generally as a function of density. The decrease, quite fast at low coverages, slows down at higher ones. We note also that all $D(\theta)$ curves in Fig. 4 for $q_F \leq 1/a$ start as convex functions of coverage already at $\theta=0$ and the characteristic *smallest* coverage at which they suffer a sudden decrease in its slope is $\theta_l=1/7$, 1/6, 1/3, and 1/2 for $q_F a=0.3$, 0.35, 0.7, and 1, respectively. In each case, the corresponding value of a/θ_l is equal to the interparticle distance l_0 (in units of a) at which the potential energy (20) with the appropriate value of q_F has the first deepest minimum in Fig. 3. For a particular oscillating interaction (i.e., particular q_F), the smallest coverage θ_l at which $D(\theta)$ ceases to be a convex function is a boundary

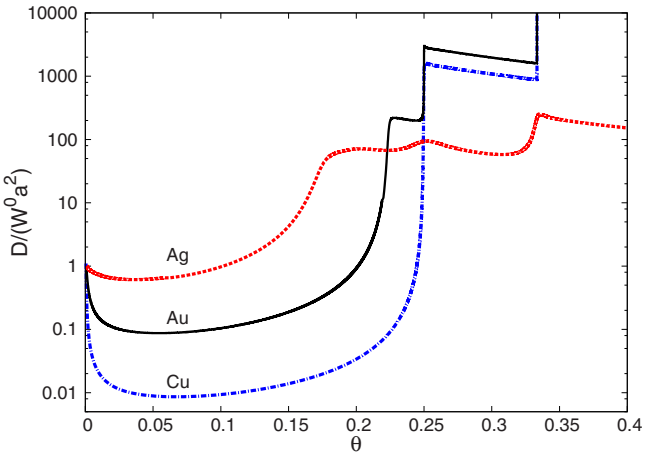

FIG. 5. (Color online) Density dependence of the diffusion coefficient divided by single particle hopping rate W_0 for Ce, Co, or Fe/Ag(111) with ϵ_F=0.41 eV, q_F=0.129 Å^{-1}, a=2.89 Å (Refs. 4, 9, 12, and 14), Co, Fe/Au(111) with ϵ_F=0.12 eV, q_F=0.173 Å^{-1}, a=2.8 Å (Ref. 4) and Ce, Cu, Ce or Fe /Cu(111) with ϵ_F =0.39 eV, q_F=0.217 Å^{-1}, a=2.56 Å (Refs. 4, 9, 12, and 25) at temperature T=39 K.

between the coverages ($\theta < \theta_l$) for which the interparticle attraction dominates and the ones ($\theta > \theta_l$) for which the repulsion does dominate.

To show how diffusion coefficient behaves in real systems we have used potentials encountered by adatoms at three different (111) metallic surfaces. These examples are plotted in Figs. 5 and 6. We have used potential parameters calculated in Ref. 4, surface lattice constants observed for adsorbed atoms and temperatures used in experiments. In each case parameter $q_F a$ is rather low, i.e., 0.55 for Cu(111), 0.48 for Au(111), and 0.37 for Ag(111). It means that l_0=4.08, 4.69, and 6.08, respectively. We show here diffusion at much lower temperatures than that in Figs. 3 and 4. Diffusion at so low temperatures changes with density by orders of magnitude; hence we plot diffusion coefficient for low densities up to (θ=0.4) only. This is density range, which is realized in experiments. As shown above characteristic behavior of the diffusion curve for particles that attract each other at some distances is decay at θ=0 and then a structureless convex function of density up to $\theta_l = 1/l_0$ (when mean interparticle distance is equal to the position of the deepest potential minimum). Above θ_l repulsion between adatoms causes an increase in the diffusion coefficient. The mechanism of such diffusive behavior lies in fact that particles create domains, in which attractive forces increase activation barriers for single particle jumps and all possible movements slow down. Such situation is true when occupation increases until all system is covered by single domain at $\theta_l = 1/l_0$. We can see that for each presented substrate wide diffusion minimum exists. It is present up to 1/6 for Ag, where l_0=6.08, 1/4 for Cu, where l_0=4.09 and very interestingly $\theta_0 \approx 0.5(1/4 + 1/5)$ for Au, where l_0=4.69, which means that in this last case system realizes ordered structure by half distances equal to 4 and half equal to 5. Wide minimum of diffusion coefficient means that for these ranges of densities particles condensate in stable domains with empty spaces between them. Mobility of single particle is W_0, much higher than mobility of particle which belongs to ordered cluster; thus each single particle immediately attaches one of the structures. Similarly all density fluctuation above domain density will decay very quickly with a rate equal to $D(\theta_l)$. In Fig. 6 we see how the differences between diffusion coefficient at θ=0, $\theta = \theta_l$ and at densities in between increase with decaying temperature, which is related to the fact that ordered domains at low temperatures are more stable.

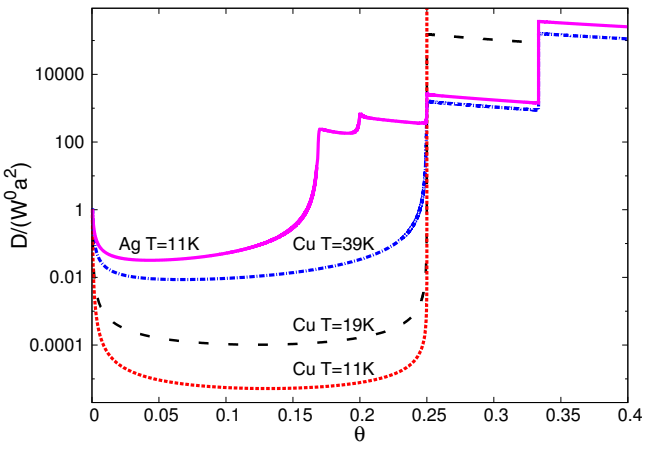

FIG. 6. (Color online) Density dependence of the diffusion coefficient divided by single particle hopping rate W_0 for Ce, Co or Fe/Ag(111) with ϵ_F=0.41 eV q_F=0.129 Å^{-1}, a=2.89 Å (Refs. 4, 9, 14, and 12) at T=11 K and Fe/Au(111) and Ce, Cu, Ce or Fe/Cu(111) with ϵ_F=0.39 eV, q_F=0.217 Å^{-1}, a=2.56 Å (Refs. 4, 9, 12, and 25) at T=39, 19, and 11 K.

Character of the interparticle interaction at closest possible separations, i.e., repulsion, attraction, or the potential energy minimum, determines the overall shape of the $D(\theta)$ dependence. For small $q_F a$'s, the particles that reside at closest possible separations from their neighbors experience the interaction induced repulsion. With increasing $q_F a$ they find themselves first at the interaction potential energy minimum, then experience attraction and then the interaction energy maximum. The cycle repeats with further increase in $q_F a$. Such a cycle of successive repulsions and attractions at a given separation should lead to a nonmonotonic dependence of the diffusion coefficient on the parameter q_F at a particular fixed coverage: we expect that after a monotonic $q_F a$ dependence of D for $q_F a$ up to about 1, the diffusion coefficient should pass through a series of minima and maxima as $q_F a$ further increases. Indeed, this is observed in Fig. 7 in which D is plotted against $q_F a$ for fixed coverage. Following the curve for $\theta = 1/6$ we observe a monotonic decrease in D until a minimum is reached for $q_F a \approx 0.7$. With further increase in $q_F a$ the maximum is reached for $q_F a \approx 0.8$, followed by a minimum around $q_F a \approx 1$, a maximum around $q_F a \approx 1.4$, and a minimum again, at $q_F a \approx 2.1$. The oscillations of D continue with increasing $q_F a$ but their amplitude decreases mirroring the decreasing amplitude of oscillations of the interaction potential energy $\varepsilon(r=\text{const})$ with increasing $q_F a$ [c.f. Eq. (20)]. For $\theta = 1/3$ the q_F dependence of D is very similar to that for $\theta = 1/6$ except that the former starts with much higher value for small $q_F a$ and has an inflection point around $q_F a \approx 0.7$ rather than a narrow minimum followed by a nar-

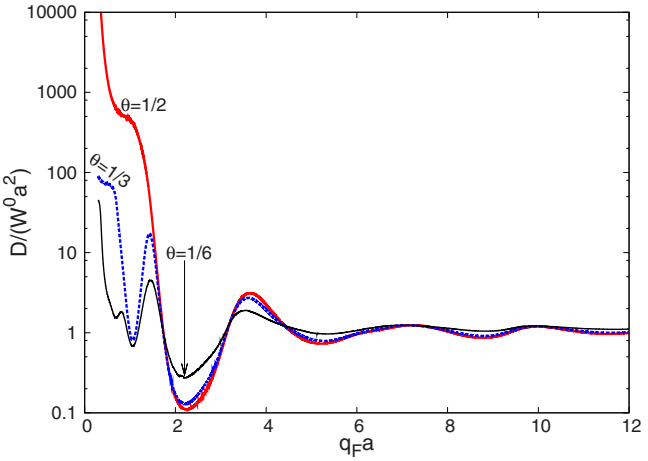

FIG. 7. (Color online) Diffusion coefficient D over single-particle mobility W_0 for $\beta=60$ eV-1 as a function of a parameter q_F of the oscillating interaction potential energy (20) with $\epsilon_F=0.36$ eV for coverages $\theta=1/6$ (thin solid line), $\theta=1/3$ (dashed line), and $\theta=1/2$ (thick solid line).

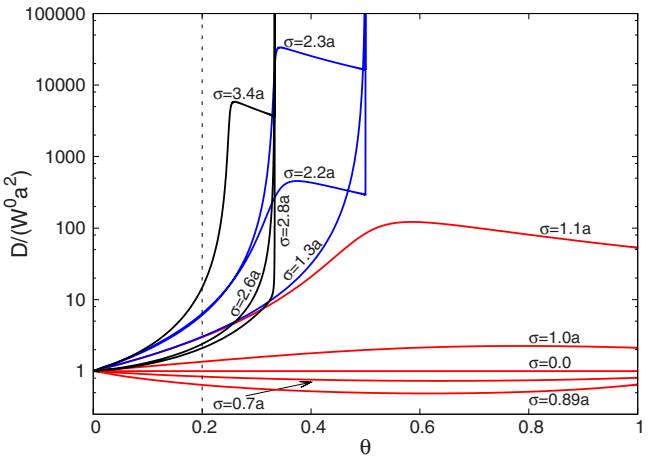

FIG. 8. (Color online) Coverage dependence of diffusion coefficient D divided by W_0 for the Lennard-Jones interparticle interaction (21) for $\beta=20$ eV^{-1}, $\epsilon_{LJ}=0.031$ eV and several values of σ.

row maximum. The same behavior shows curve with $\theta=1/2$ with inflection point at $q_Fa=1$. Beyond $q_Fa\approx 2$ all curves follow closely each other.

B. Diffusion of particles interacting via Lennard-Jones potential

Neutral particles are known to interact via long-range Lennard-Jones potential energy (21). Its repulsive core falls off more rapidly than $1/r^2$ (in fact, it falls as $1/r^{12}$, reaches an equilibrium position minimum at $r_{\min}=2^{1/6}\sigma$, and is attractive at larger distances, falling off like $1/r^6$). A staircase of ordered phases at coverages $\theta=1/n$ is supported by such an interaction (similarly like for a purely repulsive interaction), the most prominent ones being $\theta=1/2$ and 1/3, and due to huge repulsion at short distances the diffusion coefficient of particles ordered in such phases is abnormally large in comparison to that when the system is not ordered. We plot in Fig. 8 the coverage dependence of the diffusion coefficient at fixed temperature in a system with Lennard-Jones interactions corresponding to several values of σ [the other parameter in Eq. (21), ϵ_{LJ} is not varied]. The overall shape of the presented curves is determined by an interplay between two length parameters in the system: the distance $r_{\min}=2^{1/6}\sigma$ below which particles repel each other, and the substrate lattice permitted minimum separation a between interacting particles.

We can systematically analyze shapes of the $D(\theta)$ curves in Fig. 8. For $\sigma=0$ there are no interparticle interactions (except for site blocking) and $D(\theta)/W^0a^2=1$ as seen in Fig. 8. For $\sigma=0.89a$ we have $r_{\min}=a$ so when $0<\sigma<0.89a$ the interaction between particles separated by a is attractive. Consequently, it is energetically preferable for particles to be as close to each other as possible and for such values of σ the $D(\theta)$ dependence is convex (as seen for $\sigma=0.7a$ and $0.89a$ in Fig. 8), typical for systems for which the interparticle attraction dominates (c.f. Fig. 4 in Ref. 32). For $\sigma>0.89a$ the interaction at the closest separation $r=a$ becomes repulsive and, indeed, for $\sigma=a$, the $D(\theta)$ dependence becomes concave, resembling qualitatively $D(\theta)$ for weakly repulsive short range interaction in Fig. 3 of Ref. 32. With further increase in σ the repulsion at $r=a$ increases: for $\sigma=1.1a$ we note a characteristic maximum of D around $\theta=1/2$ also observed already for stronger short-range interactions in Fig. 3 of Ref. 32. For $\sigma=1.3a$ the repulsion at $r=a$ is strong enough to induce a preferential occupation of every second site (note that the interaction at the $r=2a$ separation is still weakly attractive in this case), causing the diffusion coefficient to suddenly raise by many orders of magnitude as θ approaches 1/2 from below.

With further increase in σ we reach, at $\sigma=2a/2^{1/6}=1.78a$, the point beyond which the interaction at $r=2a$ is no longer attractive. For σ somewhat larger than $1.78a$ we have a very strong repulsion at $r=a$ and a much weaker one at $r=2a$. We see in Fig. 8 that for $\sigma=2.2a$ a local maximum of $D(\theta)$ develops for $\theta\approx 1/3$, hinting at a preferential occupation of every third site around this coverage due to repulsion for $r=2a$, followed by a sharp, almost discontinuous raise of D at $\theta=1/2$ due to an extremely strong repulsion at $r=a$. With further increase in σ the repulsion at $r=2a$ becomes stronger so the structure around $\theta=1/3$ becomes as sharp as that around $\theta=1/2$. The examples are curves for $\sigma=2.3a$, $2.6a$, and $2.8a$ in Fig. 8. For the latter, however, the interaction at the separation $r=3a$ is also repulsive. In fact, with further increase in σ features similar to those around $\theta=1/2$ and 1/3 develop also around $\theta=1/4$, as seen for $\sigma=3.4a$. This is because for $\sigma>3a/2^{1/6}=2.67a$ the interaction at the separation $r=3a$ becomes repulsive and, when strong enough, it leads to a preferential occupation of every fourth site for $\theta\approx 1/4$. This structure is not present yet for $\sigma=2.8a$ at the temperature selected in Fig. 8.

The character of the coverage dependence of the diffusion coefficient changes qualitatively every time when the interaction between particles becomes repulsive at any of the interparticle separations permitted by the substrate lattice, i.e., every time when σ increases through $na/2^{1/6}$. For σ such that $n/2^{1/6}<\sigma/a<(n+1)/2^{1/6}$ the particles separated by distances $r=a,2a,\ldots,na$ repel each other (with the repulsion

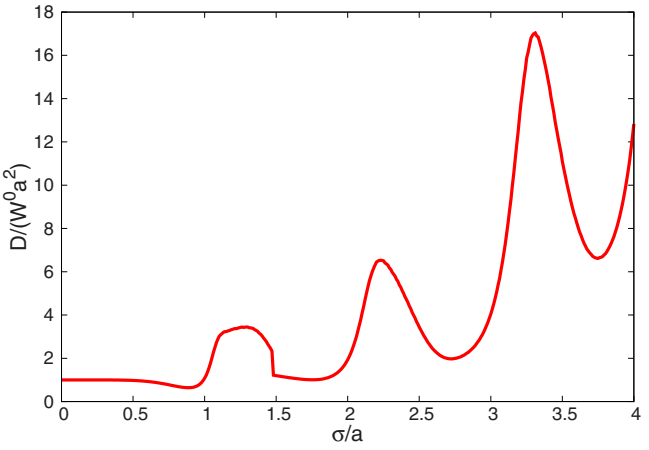

FIG. 9. (Color online) Dependence of the diffusion coefficient D divided by W_0 at $\theta=1/5$ on the Lennard-Jones interaction parameter σ for $\beta=20$ eV^{-1} and $\epsilon_{LJ}=0.031$ eV (same as in Fig. 8).

being stronger for shorter separations) while they attract each other for separations $r=(n+1)a$ and larger. In such case one expects at $T\approx 0$ a sharp increase in the diffusion coefficient at coverages $\theta=1/2,1/3,\ldots,1/(n+1)$ due to the low temperature structural organization of the adsorbate at these coverages to minimize the total interaction energy in the system. In our runs done at lowest temperatures for which the calculations are feasible we see such structures for $\theta=1/2$, 1/3, and 1/4. Still, one expects that as the parameter σ is varied one should observe a nonmonotonic oscillatory changes in the diffusion coefficient at low enough coverages. Indeed, this is seen in Fig. 9 in which $D(\theta=1/5)$ is plotted as a function of σ/a. The maxima are noted for σ/a approximately *half way* between $\sigma=na/2^{1/6}$ for $n=1,2,3,4,\ldots$, i.e., for $\sigma/a\approx 1.3,2.2,3.1,\ldots$, for which the interaction is already strongly repulsive for all interparticle separation up to $a,2a,3a,\ldots$, respectively.

IV. CONCLUSIONS

Variational approach has been applied to examine collective diffusion in a one-dimensional lattice gas systems with two type of long-range interparticle interaction: the electron-gas-mediated interaction described by the oscillating Friedel-like potential energy (20), and the Lennard-Jones interaction corresponding to the potential energy (21). We have discussed the features of the coverage (adsorbate density) dependence of the diffusion coefficient for both these interactions and compared them with those investigated in detail for purely repulsive long-range interaction[37] corresponding to the potential energy $\propto 1/r^2$ as well as with the behavior typical for short-range repulsive and attractive interactions.[32]

In general, at densities above half coverage ($\theta>1/2$), at which the interparticle repulsion at short distances plays a main role, the diffusion coefficient for the repulsive and the oscillating interaction behaves, as a function of coverage, qualitatively similarly: the diffusion coefficient is much higher than without interactions and depends on coverage relatively weakly. This is true even for the Lennard-Jones interaction, except that a very steep repulsive core in this case, making creation of a high density adsorbate energetically very costly, results in huge values of the diffusion coefficient at such densities.

At lower densities, the behavior of the coverage dependence of diffusion coefficient for the Lennard-Jones interaction, repulsive for interparticle separations $r<r_{\min}$ and attractive for $r>r_{\min}$, is quite easy to understand. At sufficiently low temperatures, it experiences for increasing θ a finite series of progressively sharper increases at "critical" coverages $\theta=1/n$ ($n=n_{\max},n_{\max}-1,\ldots,2$). The first one, for $\theta=1/n_{\max}$, corresponds to the largest interparticle distance $r=n_{\max}a<r_{\min}$ at which the interaction between the particles is still repulsive [i.e., at the separation $r=(n_{\max}+1)a>r_{\min}$ the interaction is already attractive]. As temperature increases, the structures at lower densities of this series are usually smoothed out. In fact, we observe for the Lennard-Jones interaction a delicate interplay between two length scales: the lattice constant a which determines what actual distances between particles are possible, and the characteristic length of the interaction potential, $r_{\min}$, separating the short-range repulsion from the attraction at larger distances. When $r_{\min}<a$ then the repulsive core of the interaction is irrelevant and the diffusion coefficient exhibits features similar to those observed for short-range attractive interactions.

It appears that the character of diffusion for the oscillating interactions is similar to that for particles interacting via Lennard-Jones forces. It is the position of the first deepest minimum, which decides about the boundary density θ_l up to which each diffusion curve for oscillating potential is convex. Above $\theta_l=1/l_0$ diffusion coefficient behaves similarly to this for α/r^2 potential, it has sharp jumps for each $\theta=1/n$ with n being natural number, and then it slowly decays. The existence of multiple interaction potential energy minima and, consequently, alternating regions of interparticle attraction and repulsion can only modify value of the diffusion coefficient. Such modification can be realized via static as well as kinetic part of diffusion coefficient, which means that either adsorption wells or barriers are changed by interactions. Oscillating nature of the interaction potential is more important for higher values of q_Fa, where minima and maxima are narrow and contain one lattice site only. For lower values of q_Fa (more important for real adsorbates at metallic surfaces), minima are wide and contain several lattice sites (see Fig. 3); hence it is not surprising that at low densities diffusion coefficient behaves similarly to that for Lennard-Jones potential. Structures built by attractive interparticle interactions are capable of creating local domains of ordered phases. Collective diffusion coefficient of the system built by such domains is much lower than the single-particle mobility W_0 and at low temperatures stays almost constant up to ordering density, above which is increases rapidly.

At fixed density diffusion coefficient for both interaction types oscillates as a function of the interaction characteristic length due to the interplay between the interparticle distances allowed by the substrate lattice structure and the average interparticle distances, which minimize the total interaction energy. It means that small modification of the relation between interaction constant q_F and lattice constant a can induce large change in the diffusion coefficient.

ACKNOWLEDGMENTS

This work was supported by Poland's Ministry of Science and Higher Education under Grant No. N202 042 32/1171. The authors thank Z. W. Gortel from the University of Alberta for continuing interest in the subject, discussions, and help in preparation of this manuscript.

*zalum@ifpan.edu.pl

[1] K. H. Lau and W. Kohn, Surf. Sci. **75**, 69 (1978).
[2] E. Wahlström, I. Ekval, H. Olin, and L. Wallden, Appl. Phys. A: Mater. Sci. Process. **66**, S1107 (1998).
[3] Z. Zhang, Q. Niu, and C.-K. Shih, Phys. Rev. Lett. **80**, 5381 (1998).
[4] P. Hyldgaard and M. Persson, J. Phys.: Condens. Matter **12**, L13 (2000).
[5] P. Hyldgaard and T. L. Einstein, Europhys. Lett. **59**, 265 (2002).
[6] J. Repp, F. Moresco, G. Meyer, K.-H. Rieder, P. Hyldgaard, and M. Persson, Phys. Rev. Lett. **85**, 2981 (2000).
[7] K. A. Fichthorn and M. Scheffler, Phys. Rev. Lett. **84**, 5371 (2000).
[8] A. Bogicevic, S. Ovesson, P. Hyldgaard, B. I. Lundqvist, H. Brune, and D. R. Jennison, Phys. Rev. Lett. **85**, 1910 (2000).
[9] N. Knorr, H. Brune, M. Epple, A. Hirstein, M. A. Schneider, and K. Kern, Phys. Rev. B **65**, 115420 (2002).
[10] V. S. Stepanyuk, A. N. Baranov, D. V. Tsivlin, W. Hergert, P. Bruno, N. Knorr, M. A. Schneider, and K. Kern, Phys. Rev. B **68**, 205410 (2003).
[11] Y. Tiwary and K. A. Fichthorn, Phys. Rev. B **75**, 235451 (2007).
[12] N. N. Negulyaev, V. S. Stepanyuk, L. Niebergall, P. Bruno, M. Pivetta, M. Ternes, F. Patthey, and W.-D. Schneider, Phys. Rev. Lett. **102**, 246102 (2009).
[13] T. Yokoyama, T. Takahashi, K. Shinozaki, and M. Okamoto, Phys. Rev. Lett. **98**, 206102 (2007).
[14] A. Schiffrin, J. Reichert, W. Auwarter, G. Jahnz, Y. Pennec, A. Weber-Bargioni, V. S. Stepanyuk, L. Niebergall, P. Bruno, and J. V. Barth, Phys. Rev. B **78**, 035424 (2008).
[15] H. F. Ding, V. S. Stepanyuk, P. A. Ignatiev, N. N. Negulyaev, L. Niebergall, M. Wasniowska, C. L. Gao, P. Bruno, and J. Kirschner, Phys. Rev. B **76**, 033409 (2007).
[16] E. Bussmann, S. Bockenhauer, F. J. Himpsel, and B. S. Swartzentruber, Phys. Rev. Lett. **101**, 266101 (2008).
[17] N. N. Negulyaev, V. S. Stepanyuk, W. Hergert, P. Bruno, and J. Kirschner, Phys. Rev. B **77**, 085430 (2008).
[18] J. Lagoute, X. Liu, and S. Fölsch, Phys. Rev. B **74**, 125410 (2006).
[19] C. Liu, T. Uchihashi, and T. Nakayama, Phys. Rev. Lett. **101**, 146104 (2008).
[20] I. Fernandez-Torrente, S. Monturet, K. J. Franke, J. Fraxedas, N. Lorente, and J. I. Pascual, Phys. Rev. Lett. **99**, 176103 (2007).
[21] F. Silly, M. Pivetta, M. Ternes, F. Patthey, J. P. Pelz, and W.-D. Schneider, Phys. Rev. Lett. **92**, 016101 (2004).
[22] N. N. Negulyaev, V. S. Stepanyuk, L. Niebergall, W. Hergert, H. Fangohr, and P. Bruno, Phys. Rev. B **74**, 035421 (2006).
[23] J. M. Rogowska and M. Maciejewski, Phys. Rev. B **74**, 235402 (2006).
[24] V. S. Stepanyuk, L. Niebergall, R. C. Longo, W. Hergert, and P. Bruno, Phys. Rev. B **70**, 075414 (2004).
[25] V. S. Stepanyuk, N. N. Negulyaev, L. Niebergall, R. C. Longo, and P. Bruno, Phys. Rev. Lett. **97**, 186403 (2006).
[26] D. A. Reed and G. Ehrlich, Surf. Sci. **102**, 588 (1981).
[27] R. Gomer, Rep. Prog. Phys. **53**, 917 (1990).
[28] A. Danani, R. Ferrando, E. Scalas, and M. Torri, Int. J. Mod. Phys. B **11**, 2217 (1997).
[29] T. Ala-Nissila, R. Ferrando, and S. C. Ying, Adv. Phys. **51**, 949 (2002).
[30] Z. W. Gortel and M. A. Załuska-Kotur, Phys. Rev. B **70**, 125431 (2004).
[31] M. A. Załuska-Kotur and Z. W. Gortel, Phys. Rev. B **72**, 235425 (2005).
[32] L. Badowski, M. A. Załuska-Kotur, and Z. W. Gortel, Phys. Rev. B **72**, 245413 (2005).
[33] M. A. Załuska-Kotur, Ł. Badowski, and Z. W. Gortel, Physica A **357**, 305 (2005).
[34] M. A. Załuska-Kotur and Z. W. Gortel, Phys. Rev. B **76**, 245401 (2007).
[35] F. Krzyżewski and M. A. Załuska-Kotur, Phys. Rev. B **78**, 235406 (2008).
[36] M. Yakes, M. Hupalo, M. A. Załuska-Kotur, Z. W. Gortel, and M. C. Tringides, Phys. Rev. Lett. **98**, 135504 (2007).
[37] M. A. Załuska-Kotur and Z. W. Gortel, Phys. Rev. B **74**, 045405 (2006).
[38] V. V. Slavin and A. A. Slutskin, Phys. Rev. B **54**, 8095 (1996).
[39] P. Bak and R. Bruinsma, Phys. Rev. Lett. **49**, 249 (1982).